JOURNAL OF PROPULSION AND POWER
Vol. 11, No. 2, March–April 1995

Space Shuttle Simplified LO2 Check Valve Development Tests

Michael J. Barrett* and Gregory S. Aber*
NASA Johnson Space Flight Center, Houston, Texas 77058
and
Timothy W. Reith†
Rockwell International Corporation, Houston, Texas 77058

The coil spring in a Space Shuttle liquid oxygen check valve failed due to cyclic fatigue in September, 1991. The dual-flapper, swing check valve is used to prevent reverse flow to the Space Shuttle Main Engines. Upon inspection of the failed component, the spring tangs were found to be missing and heavy wear was observed on the i.d. of the spring coils. The fracture surfaces revealed that the metal had been steadily worn away until a simple overload caused the final fracture. A series of flow tests using water and a water/gas mixture was conducted to identify the flow phenomenon that produced the cyclic wear. A Plexiglas® outlet housing was utilized to view the flapper behavior under different flow conditions and to aid in high-speed photography. The tests revealed that flow instabilities induced two oscillatory flapper responses: 1) a rocking mode and 2) a chattering mode. Initially, attempts were made to reduce the spring-flapper oscillations. However, the final solution to the problem was a springless configuration that satisfied the valve's design requirements and eliminated the oscillations. The springless design relied on the inherent ability of the reverse flow momentum to close the flappers.

Introduction

THE Space Shuttle Main Propulsion System (MPS) utilizes liquid hydrogen (LH2) and liquid oxygen (LO2) as propellants. The LO2 system consists of fill and drain lines, engine feedlines, and bleed return lines used for thermal conditioning of each Space Shuttle Main Engine (SSME) prior to ignition. The bleed lines are also used for pogo suppression during SSME mainstage operation. During entry, the LO2 lines and SSMEs are purged with helium to maintain a positive system pressure that reduces the possibility of ingesting contaminants. The LO2 bleed check valve (BCV) is located in the engine bleed line between the SSME and the LO2 17-in. manifold (see Fig. 1). If a SSME experiences a preliminary or uncontained shutdown during flight, the BCV prevents LO2 flow from the manifold to the engine. During entry, the LO2 manifold is pressurized and helium is supplied to the engine through a 0.052-in.-diam orifice in the BCV. The orifice limits the helium consumption during the SSME purge. If the BCV fails to close during entry, the helium supply will be depleted prematurely, which reduces other environmental purges of Orbiter compartments. In September, 1991, helium usage during STS-43 entry operations was larger than normal onboard the Atlantis. Postflight checkout revealed that the engine-three LO2 BCV had failed open.

Current LO2 Bleed Check Valve

Valve Design

The MPS LO2 bleed check valve is a swing-style check valve. The valve has two semicircular flappers that rotate on a cylindrical hinge pin and are loaded by a coil spring (see Fig. 2). The dual flapper design provides a redundant flow passage in the event that one flapper fails closed. The valve housing is 8 in. long and is axisymmetric in the flow direction. The inlet has a 1 in. diameter that increases to 2 in. immediately downstream of the flapper seat, and then returns to 1 in. at the valve outlet. The internal flow is not axisymmetric due to the crossflow flapper bridge and flapper assembly.

The valve housing, hinge pin, and Teflon®-coated flappers are all made of corrosion-resistant stainless steel. The flapper seat is made of a nickel-chromium-iron alloy. The spring metal is a nickel-cobalt alloy that provides a fairly stable spring constant across the operating temperature band.

The design specifications for the BCV call for a maximum pressure drop Δp of 1.2 psid with LO2 flow through both passages totaling 4 lb/s. The allowable Δp for a single passage is 3.2 psid at the same flow rate. A typical flow rate during SSME prelaunch conditioning is approximately 5.5 lb/s. To satisfy the SSME thermal requirements, an allowable Δp of 2.3 psid is also specified at 5.5 lb/s of LO2 flow.[1]

Failure Description

Scanning electron microscopy (SEM) performed on the STS-43 spring revealed that nearly 50% of some coil cross sections

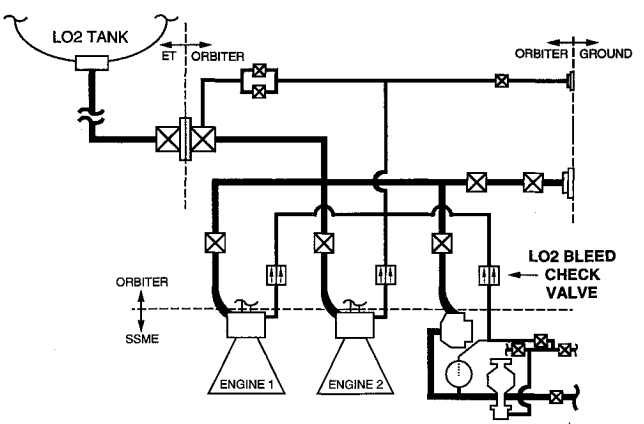

Fig. 1 Space Shuttle Main Propulsion liquid oxygen feed and return system.

Presented as Paper 93-2486 at the AIAA/SAE/ASME/ASEE 29th Joint Propulsion Conference and Exhibit, Monterey, CA, June 28–30, 1993; received Nov. 9, 1993; revision received June 16, 1994; accepted for publication July 12, 1994.

*Test Engineer, Propulsion Test Section, Propulsion and Power Division. Member AIAA.

†Propulsion Engineer, Space Systems Division, 555 Gemini Ave. Member AIAA.

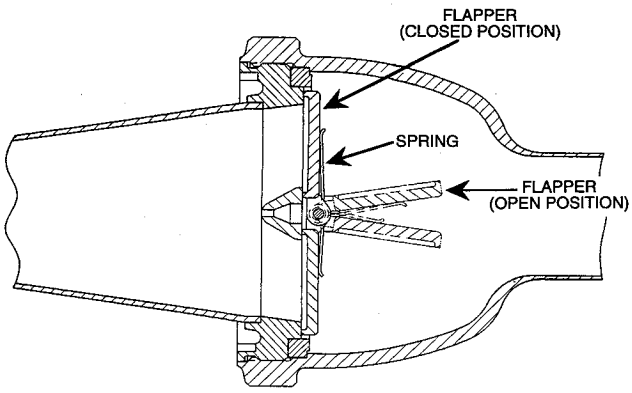

Fig. 2 Current BCV design.

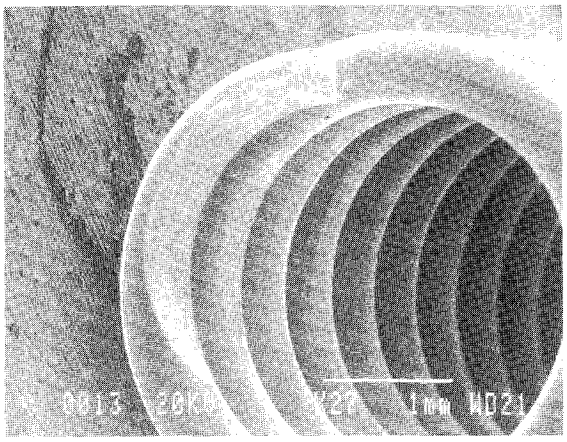

Fig. 3 SEM photograph of spring wear and fracture.

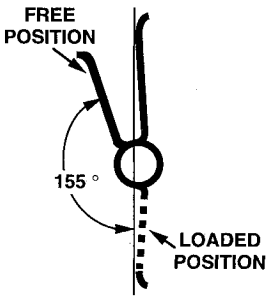

Fig. 4 Coil spring load.

had worn away (see Fig. 3). The reduced cross section led to higher stresses and caused fatigue crack propagation on the tension side of the coil wire. The final fracture was caused by a simple overload at the base of the spring tang.[2]

In the installed position, the spring is loaded even when the flappers are closed (see Fig. 4). The i.d. of the coil contacts the upstream side of the flapper pin due to the spring tangs and loop pushing on the downstream side of the flappers. When the flappers are opened, the force applied to the pin by the coil increases. If the flappers are then placed in a cyclic mode, the friction between the spring and pin steadily wears the spring coils until the spring fails. This is precisely what happened to the BCV removed from the Atlantis. As an interim corrective action, the number of flights each spring that could be flown was limited to four. This restriction was imposed until a permanent solution to the spring wear could be implemented.

Water Flow Tests

Following the metallurgical analysis, a series of water flow tests was performed. The purpose of the flow tests was two-fold: first, to determine the flow phenomenon responsible for the cyclic wear, and second, to gain insight into possible design changes that would eliminate the spring wear.

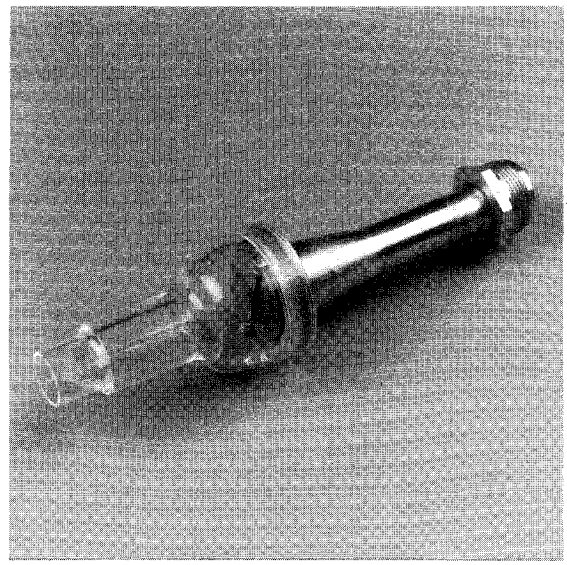

Fig. 5 BCV test article with Plexiglas outlet.

Current Valve Configuration

The objective of the first water flow test series was simply to reproduce the oscillatory behavior that caused the spring fatigue. The test article was a version of the flight BCV that did not have the purge orifice. However, the significance of a 0.052-in. orifice in the center of the flapper bridge was considered to be small when examining the overall flow characteristics around the flappers. In order to observe the area downstream of the flapper seat, an outlet housing was machined out of Plexiglas. The test article is shown in Fig. 5.

Because of the large difference in kinematic viscosities between LO2 and water,[3-5] no attempt was made to simulate the Reynolds number of the flight flow. However, since the flight Reynolds number is so large, the flow regime is fully turbulent and the viscous effects were assumed to be negligible when considering the flowfield momentum balance.[6] Therefore, the test flow rates were chosen to simulate the dynamic pressures that are experienced during flight operations. The pressure drop data obtained was displayed using equivalent LO2 flow rates based on the dynamic pressure similarity.[7]

During ascent, the BCV is exposed to a two-phase mixture of gaseous and liquid oxygen. For the investigative flow tests, a two-component mixture of water and gaseous nitrogen (GN2) at various void fractions was used in an attempt to envelop the ascent two-phase conditions. The results of the two-component flow tests were used only for qualitative comparisons to the single-phase water tests.

The initial test system consisted of a 1500-gal deionized water tank, a GN2 injection system for two-component flow tests, and a dye injection system for flow visualization. The water flow rate was controlled via a throttle valve located upstream of the BCV and was measured using a turbine flow meter. To obtain the different void fractions during two-component flow tests, the GN2 flow rate was also controlled via a throttle valve and was measured using a variable area flow meter. The gas injection point was placed downstream of the turbine flow meter so as not to disturb the water flow rate measurement. The dye injection system consisted of a pressure-fed tank, a throttle valve to control the amount of dye injected, and a $\frac{1}{8}$-in.-diam tube placed centrally in the main flow tube to serve as an injector. A differential pressure transducer measured the Δp across the BCV that was mounted in the test stand with the flow axis horizontal. Video and high-

speed photography were used extensively to document test results.

After completion of the first series of tests, two oscillatory modes of flapper response were successfully identified. At the lower water flow rates, the flappers would open symmetrically and then rock from the seat of one to the seat of the other as one rigid unit (see Fig. 6). As the water flow rate was increased, the flappers continued to open, but began to oscillate independently of one another, or chatter, as shown in Fig. 7. During two-component flow tests, the flappers exhibited a more severe chattering behavior that caused the flappers to repeatedly impact the seat area. Both the rocking and chattering modes were capable of inducing spring wear due to friction between the spring and the flapper pin.

The Δp data for the spring-flapper configuration was compared to the qualification data previously recorded for the check valve.[8] The valve qualification tests had been performed using liquid nitrogen (LN2) and the same test unit. Figures 8 and 9 illustrate that, instead of Reynolds number, the simulation of dynamic pressure was appropriate in order to obtain the correct resistance coefficient, K ($K = \Delta p/p_{dyn}$).[7] The water flow data yielded resistance coefficients, or LO2 Δp predictions, which were slightly higher than the original qualification data. This can be seen in Fig. 9. However, the prediction trends were similar and suggested that a fixed pressure bias might be present. The most likely source of bias in the Δp prediction is the calculation of the test stand pressure loss due to inlet and outlet fitting assemblies. For both the water and LN2 tests, the fitting pressure loss was calculated by comparing a tare tube measured Δp, with the predicted Δp based on the solution of the Colebrook equation.[5] The difference in the measured and predicted Δp values was attributed to a flow resistance associated with the test stand interface fittings. The pressure drop due to the fittings was subtracted from the pressure drop measured at the same flow rate with the BCV to obtain the corrected Δp value. Since the fitting pressure loss is subtracted from the measured Δp in both the qualification test data and the water flow test data, inaccuracies in the determination of fitting pressure loss would appear in the comparison between the two data sets. Since the water flow Δp results were conservative when compared to the qualification data, the test methods were considered adequate for the investigation at hand.

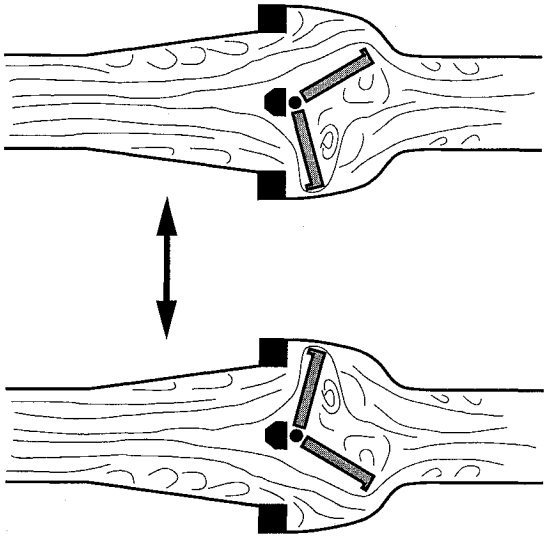

Fig. 6 Flapper "rocking" mode.

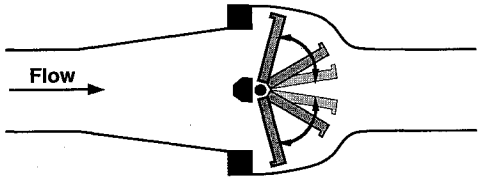

Fig. 7 Flapper "chattering" mode.

Belleville Washers/Stop Rod

The objective of the second series of flow tests was to determine if the flapper oscillations could be eliminated by minor alterations to the current design. Hardware changes that would minimize the amount of requalification testing required and maximize the utilization of existing flight hardware were strongly desired. Two hardware modifications were examined: first, the addition of Belleville washers between the flapper hinges and the hinge pin brackets in an attempt to frictionally damp the oscillations, and second, the installation of a stop rod downstream of the flappers to restrict the flapper opening travel. Both configurations were tested using the same flow conditions as those used for the spring-flapper test series. Also, the same test setup used for the first series of water flow tests was used in the second series of water flow tests.

The addition of the Belleville washers proved to be incapable of significantly reducing the flapper oscillations. Due to geometric restrictions, the amount of frictional load required to damp the flappers could not easily be obtained using Belleville washers. The introduction of an excessive frictional resistance that could cause the flappers to stick open was also a concern with this method.

Two different stop rod positions were tested (see Fig. 10). The stop rod was able to eliminate the oscillations in the higher, fully liquid flows. However, at low flow rates and in the gas-liquid flows the stop rod was ineffective. The flappers

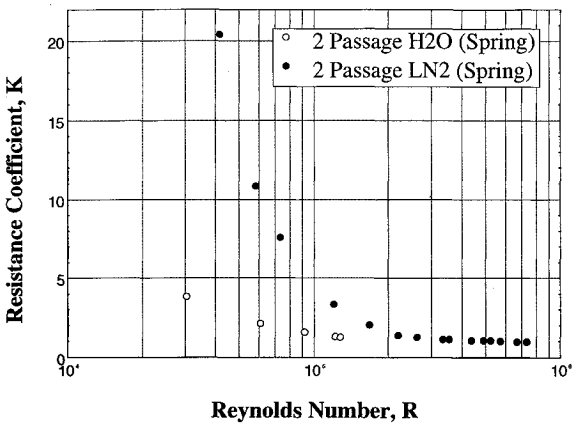

Fig. 8 Resistance coefficient vs Reynolds number for spring and flapper configuration.

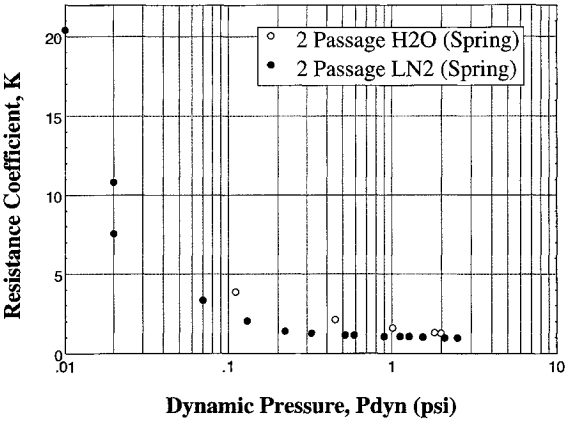

Fig. 9 Resistance coefficient vs dynamic pressure for spring and flapper configuration.

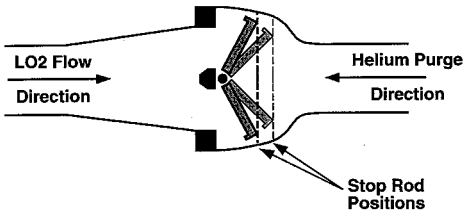

Fig. 10 Flapper stop rod positions.

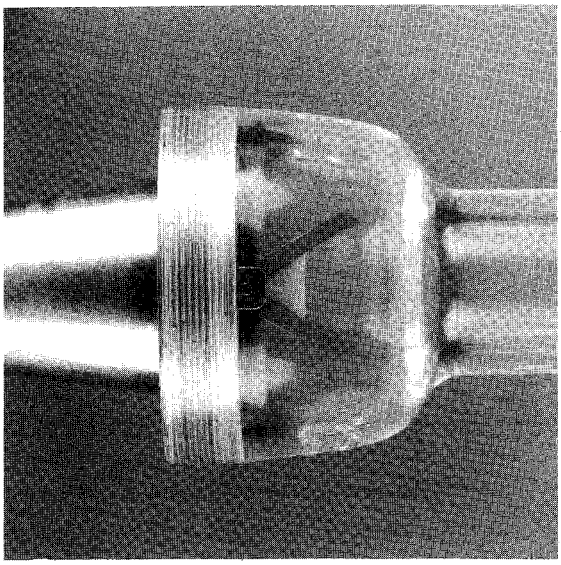

Fig. 11 Teflon flapper wedge installed.

were not held open against the stop rod and the oscillations were still present. Additionally, if the stop rod had been moved close enough to the flapper seat to eliminate the oscillations under all flow conditions, the resulting Δp across the valve would have been unacceptable.

Observations of the stop rod tests led to the suggestion of removing the spring, restricting the flapper opening travel, and allowing the reverse flow momentum to cause the valve to close when necessary. This "springless" concept was explored using a flapper wedge.

Wedge (Springless) Forward Flows

A Teflon flapper wedge was installed over the existing flapper pin in lieu of the spring as shown in Fig. 11. The wedge configuration included tabs that inserted into an existing cutout in the flapper bridge (see Fig. 12). These tabs prevented the wedge from rotating on the flapper pin, thereby limiting the opening angle of the flappers. The cutout section between the tabs was necessary to maintain an unrestricted flow path to the 0.052-in. purge orifice in the center of the flight valve. Two wedge angles, 30 and 60 deg, were chosen based on the Δp data from the stop rod tests. Using the same facility setup and test conditions as in the previous tests, the springless configuration was examined using both wedge angles.

The primary objectives of the wedge forward flow testing were to verify that either wedge would be compatible with the current valve design and to gather pressure drop data for both wedge angles. Integration of either wedge was accomplished simply by disassembling the valve, removing the spring, installing the wedge, and reassembling the valve.

No flapper oscillations were observed in any of the wedge forward flow tests. This proved that the oscillations had been caused by spring and flow force interactions and not simply by pressure fluctuations acting on the flappers. The resulting Δp data is presented in Figs. 13–15. Figures 13 and 14 show that both the 30- and 60-deg wedges satisfied the dual passage and single passage pressure drop requirements that were spec-

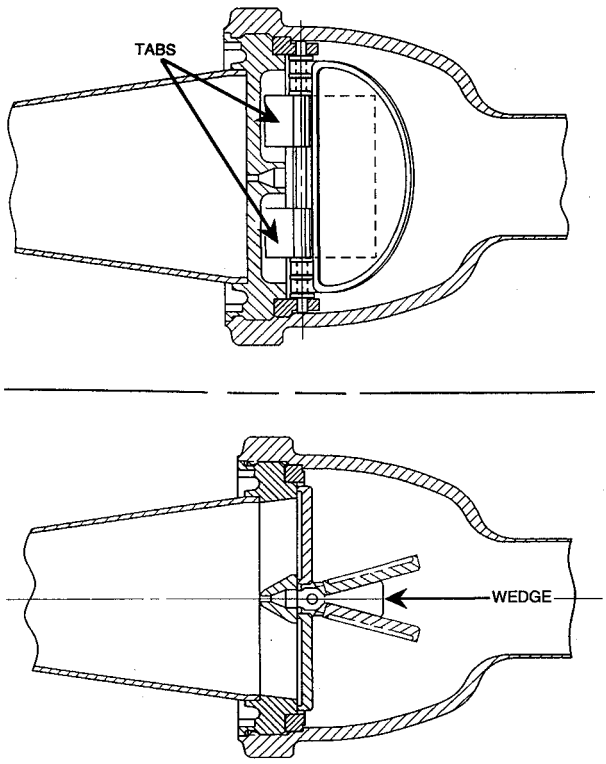

Fig. 12 Flapper wedge configuration.

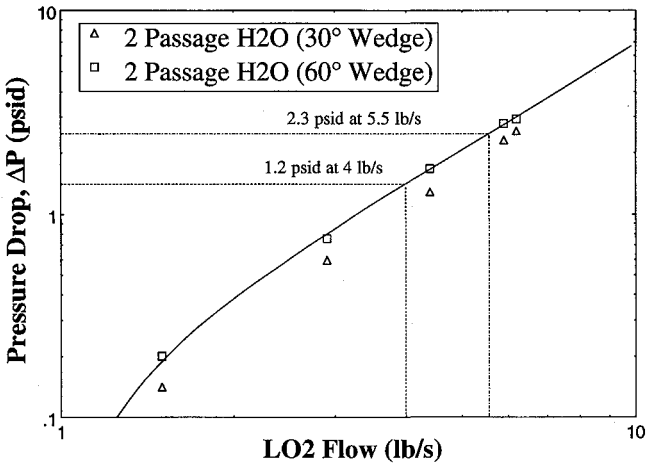

Fig. 13 Pressure drop vs equivalent LO2 mass flow for 30- and 60-deg wedge configurations.

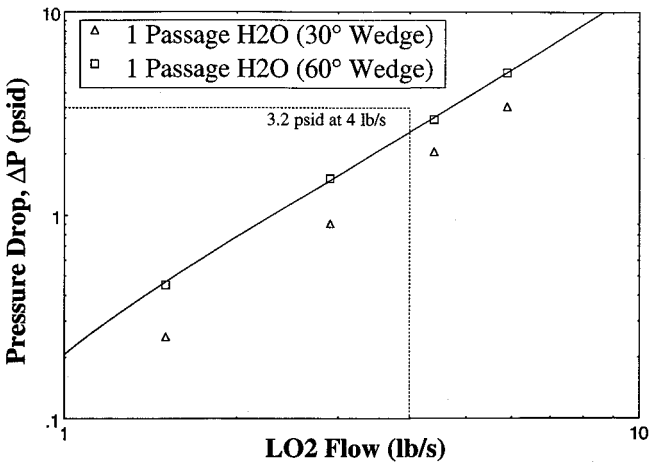

Fig. 14 Pressure drop vs equivalent LO2 mass flow for 30- and 60-deg wedge configurations.

Table 1 Reverse flow required to close flappers

Wedge angle, deg	Valve orientation	Flapper pin orientation	H2O flow, lb/s	GHe flow, SCFM
30	Horizontal	Vertical	0.13	10.5
	Horizontal	Horizontal	0.35	30.4
	Vertical	N/A	0.50	41.9
60	Horizontal	Vertical	0.13	10.5
	Horizontal	Horizontal	0.29	26.6
	Vertical	N/A	0.49	41.9

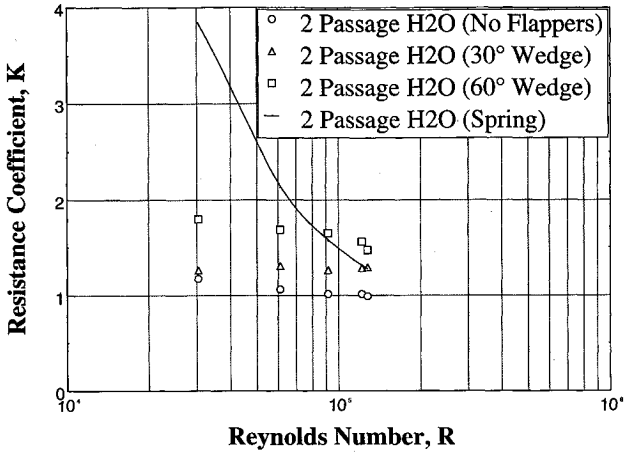

Fig. 15 Resistance coefficient vs Reynolds number for all configurations.

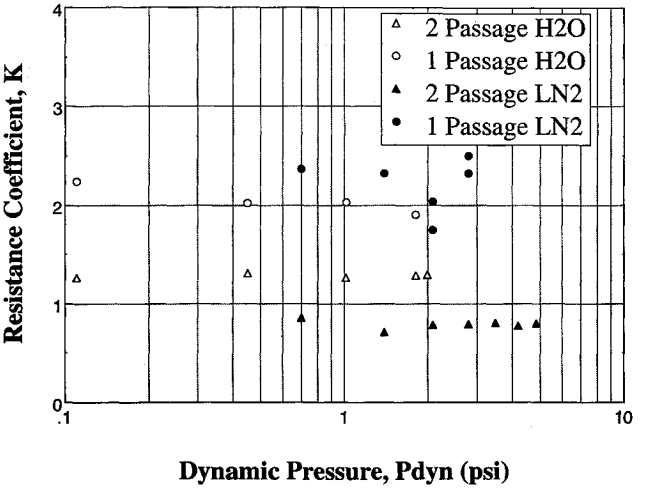

Fig. 16 Resistance coefficient vs dynamic pressure for 30-deg wedge configuration.

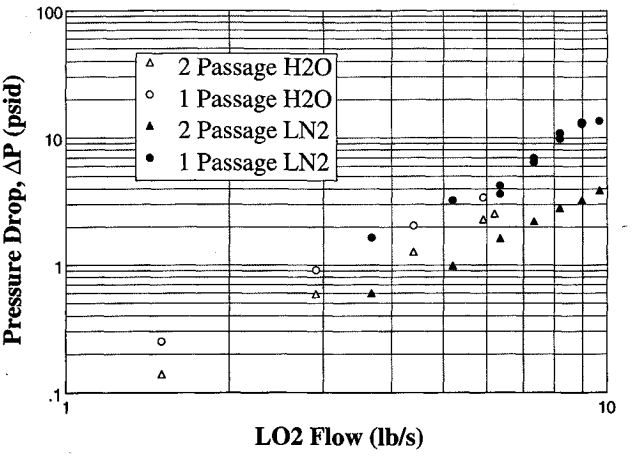

Fig. 17 Pressure drop vs equivalent LO2 mass flow for 30-deg wedge configuration.

ified earlier. Figure 15 compares the observed resistance coefficients for all of the configurations tested in the water flows. The results are as expected. As the wedge angle is increased, the flow area diminishes generating a larger resistance coefficient. The resistance coefficient for a fixed flow geometry is roughly constant because of the magnitude of the Reynolds number corresponding to each flow rate tested. The solid line in Fig. 15 shows the variable resistance associated with the change in flow area when the spring is installed. Note that the 30-deg wedge and the spring result in approximately the same flow resistance at the highest flow rates. The case with the flappers removed shows the flow resistance due to the valve housing alone. No wedge angles smaller than 30 deg were tested since the resistance due to the housing contour was comparable to the total resistance with the 30-deg wedge installed. No problems were encountered with either wedge installation in the existing valve housing. After the forward flow tests were successfully completed, the primary question that remained was whether or not the reverse flows would be capable of closing the flappers without the spring.

Wedge (Springless) Reverse Flow Tests

A final test series was conducted in order to verify that the springless BCV reverse flow requirements were acceptable for the propulsion system operational performance. The two previously mentioned scenarios requiring BCV closure are 1) an early engine out during ascent and 2) a nominal entry with environmental purges.

The 30- and 60-deg wedges were tested with the valve mounted in three different orientations: 1) flow axis horizontal with flapper pin horizontal, 2) flow axis horizontal with flapper pin vertical, and 3) flow axis vertical with flapper pin horizontal (flappers hanging down). These three valve orientations account for all possible valve orientations on the vehicle during a mission. In each orientation, the amount of reverse flow necessary to close the flappers was measured using both water and gaseous helium.

The test stand was modified to accommodate this test series. The variable area flow meter was replaced with a thermal mass flow meter to obtain a more accurate gas flow rate measurement and to provide an analog output for recording on a strip chart. The turbine flow meter and differential pressure transducer outputs were routed to a strip chart to assure that the reverse flow conditions required to close the flappers were accurately measured. Plumbing changes were made to enable valve mounting in the three required orientations.

The results of the reverse flow tests are shown in Table 1. In all cases, the flow rates measured were acceptable for usage on the Orbiter.

Flight Certification

The new BCV flight configuration utilizes a 30-deg wedge made from 304L stainless steel. The impact of the springless check valve on MPS ground turnaround operations was assessed and no problems were identified. After the develop-

ment tests were complete, qualification testing of the springless BCV was performed. The qualification tests used LN2 for the forward flow tests and both LN2 and helium to verify the reverse closure. A comparison of the qualification LN2 forward flow tests[9] and the water flow development tests is presented in Figs. 16 and 17. The qualification tests verified that the springless BCV satisfied the necessary pressure drop requirements. The reverse flow closure capability was also reaffirmed by the qualification tests. The springless BCV first flew on Space Shuttle mission STS-61 in December, 1993. The valve performed nominally and has successfully flown on all subsequent missions.

Conclusions

1) The oscillations that caused the spring to wear were caused by the interaction of the spring and flow forces on the flappers.

2) The removal of the spring from the check valve eliminated the oscillations as well as the fatigue-sensitive part.

3) The springless check valve was capable of meeting forward Δp specifications as well as reverse flow closure requirements.

4) The springless check valve option provided a simple solution making use of the current flight hardware.

5) The reliance on reverse flow momentum for check valve closure is a valid concept.

Acknowledgments

The authors sincerely thank Seshu Vaddey and Michael Burghardt of Rockwell International Space Systems Division, Houston, Texas, and Kathleen Marquardt of Lockheed Engineering and Sciences Company, Houston, Texas, for their contributions and assistance.

References

[1]Olivas, U., "Valve, Dual Check," NASA MC284-0515, Sept. 1976.

[2]Sueme, D. R., "Failure Analysis of LO2 Bleed Check Valve from OV-104," Rockwell International Space Systems Div., IL284-204-91-199, Downey, CA, Nov. 1991.

[3]Barron, R. F., *Cryogenic Systems*, 2nd ed., Oxford Univ. Press, New York, 1985, p. 479.

[4]Timmerhaus, K. D., and Flynn, T. M., *Cryogenic Process Engineering*, Plenum, New York, 1989, p. 564.

[5]Murdock, J. W., "Mechanics of Fluids," *Marks' Standard Handbook for Mechanical Engineers*, 8th ed., edited by T. Baumeister, McGraw-Hill, New York, 1978, pp. 3-33–3-70.

[6]Schlichting, H., *Boundary Layer Theory*, McGraw-Hill, New York, 1979, pp. 70–82, 596–634.

[7]"Flow of Fluids Through Valves, Fittings, and Pipe," Crane Co., TP 410, King of Prussia, PA, 1988.

[8]Wilder, P., "Qualification Test Report—Valve Dual Check," Parker Hannifin Air and Fuel Div., QTR5760024, Irvine, CA, May 1978.

[9]Marchisio, M. J., "LO2 Dual-Passage Bleed Check Valve Qualification Test," Rockwell International Space Systems Div., SSD93D0376, Downey, CA, Aug. 1993.